Periodic conductance fluctuations and lead-induced scarring in open quantum dots

1997 J. Phys.: Condens. Matter 9 5935

(http://iopscience.iop.org/0953-8984/9/27/020)

J. Phys.: Condens. Matter **9** (1997) 5935–5950. Printed in the UK PII: S0953-8984(97)82561-1

Periodic conductance fluctuations and lead-induced scarring in open quantum dots

J P Bird†§, R Akis‡, D K Ferry‡, Y Aoyagi† and T Sugano†

† Nanoelectronic Materials Laboratory, Frontier Research Program, RIKEN, 2-1 Hirosawa, Wako, Saitama 351-01, Japan

‡ Nanostructures Research Group, Center for Solid State Electronics Research, Arizona State University, Tempe, AZ 85287-6206, USA

Received 13 March 1997

Abstract. We consider the nature of ballistic electron transport in open mesoscopic cavities, coupled to external reservoirs by means of few-mode quantum point contacts. The devices vary in size over a wide range and the discrete nature of their electronic energy spectrum is expected to strongly influence the resulting electrical behaviour. Electron interference is also an important process in these devices and is investigated through studies of their low-temperature magneto-resistance. This is found to be characterized by regular fluctuations, which numerical simulations reveal to be associated with periodically recurring wavefunction scarring. Further analysis shows that the scarring is established by the collimating action of the injecting point contact, the quantum mechanical nature of which ensures that just a few cavity modes are excited to participate in transport. We therefore conclude that chaotic scattering is suppressed in mesoscopic cavities once their discrete quantum mechanical nature becomes resolved. Transport then instead occurs via a small number of regular orbits, which are stabilized by the role of the quantum point contact leads and the discrete quantization within the cavity itself. These long orbits give rise to well defined wavefunction scarring with measurable magneto-transport results.

1. Introduction

Recent interest in the electrical properties of semiconductor quantum dots has been stimulated by their potential application as a novel experimental probe of quantum chaos [1, 2]. While precise details differ between experiment, the devices used in these studies generally consist of some mesoscopic cavity which is connected to external reservoirs by means of one-dimensional lead openings [3–9]. The central cavity itself is defined on a spatial scale comparable to the fundamental length scales of the electron, while its shape is essentially determined by lithographic considerations [10, 11]. In particular, the use of high mobility semiconductor material ensures that electronic motion within the cavity is predominantly ballistic. Furthermore, at temperatures below a few degrees Kelvin phase coherence of the trapped electrons may be maintained over very long time scales [4, 7]. Under such conditions, electron interference is found to be an important process in determining the electrical properties of these quantum devices and the details of the interference are expected to reflect the ballistic motion of electrons within the cavity.

§ Address as at 1 August 1997: Center for Solid State Electronic Research, Arizona State University, Tempe, AZ 85287-6206, USA.

0953-8984/97/275935+16$19.50

The one-dimensional lead openings which connect the central dot to the source and drain regions are typically realized using quantum point contacts, the number of propagating modes in which can be varied continuously. In most experiment, the leads are operated in the few mode regime where the discrete quantum mechanical nature of the openings is strongly resolved. Electrons incident from the external reservoirs are then only able to enter the cavity by matching their transverse momentum component with the quantized values within the contact itself. This process results in collimation of the incoming electrons, which are therefore injected into the cavity in a highly directed beam with a narrow angular spread [12–14]. In sufficiently small cavities, the discrete nature of the electronic energy spectrum may also remain resolved, even in the presence of the continuous current flow [15, 16]. With the collimation provided by the input point contact and the discrete nature of the cavity eigenvalues the transport should be dominated by highly regular behaviour, even in devices in which the corresponding classical motion of particles is known to be chaotic [14]. Such behaviour is quite distinct to the chaotic scattering expected in ballistic quantum dots, when their lead openings are adjusted to support a large number of modes [17–20]. In this regime, the point contacts essentially act as classical entities and evidence for geometry induced chaos has been observed in experiment [5]. Consequently, it is of interest to study how the suppression of chaos occurs in mesoscopic cavities, as their size is reduced and the quantum mechanical nature of their leads also becomes resolved.

In this report, we discuss the results of experimental studies of ballistic electron transport in strongly confined open quantum dots. The number of modes occupied in the leads typically ranges between one and five in the course of experiment, corresponding to the few-mode quantum regime mentioned above. The devices themselves vary in size over a wide range and the discrete nature of their electronic energy spectrum is expected to strongly influence the resulting electrical behaviour. Electron interference is also an important process in these devices and is investigated through studies of the reproducible fluctuations in their low-temperature magneto-resistance [3, 4, 6–9]. The fluctuations are found to exhibit strikingly periodic characteristics which persist over a wide range of magnetic field and gate voltage, suggesting that interference in these discrete quantum dots is dominated by a small family of stable orbits. Consistent with this conclusion, numerical simulations of the devices are found to reveal marked scarring of the total wavefunction, which is produced by a small group of semi-classical orbits [12]. The scarring is found to result from a build-up of constructive interference between electrons, coherently stored within the cavity over very long time scales. This result is consistent with experiment, where an exponential damping of the fluctuation amplitude is obtained as the temperature is increased. Further numerical analysis shows that the scarring is established by the collimating action of the injecting point contact, the quantum mechanical nature of which ensures that just a few cavity modes are excited to participate in transport. In this sense, the coupling between the point contacts and the dot is similar to that in resonant tunnelling diodes, in which only those modes which couple effectively through the tunnel barriers are excited and exhibit scars [21, 22]. Consequently, theoretical treatments which express the conductance as a uniform sum over all possible paths between the input and output will fail to satisfactorily account for the observed behaviour [17–20]. Instead, our results demonstrate that the correct semi-classical description of interference in these quantum devices is one in which just a small number of orbits is preferentially excited by the injecting lead.

The organization of this paper is as follows. In section 2, we discuss the details of the device fabrication and their basic characterization. Our main experimental results are then presented in section 3, while section 4 compares these results with quantum mechanical

simulations of electronic transport. The implications of this comparison are further discussed in section 5, where we also present our final conclusions.

2. Device details and experimental techniques

Table 1 summarizes the low-temperature characteristics of the eight split-gate quantum dots we study here and defines the labelling scheme we employ. The devices were fabricated in GaAs/AlGaAs heterojunction material, with electron beam lithography used to define the fine line pattern of the gates (figure 1(a), right inset). Transport through the resulting square cavities is highly ballistic in nature and here we focus on the behaviour obtained when the number of propagating modes in the leads varies between roughly one and five. In this few-mode regime, momentum conservation results in electrons being injected into the cavity in a collimated beam, rotated away from the point contact axis [12] (see later). The gate design we study is therefore highly efficient in trapping electrons and experimental studies suggest a storage time of the order of several hundred pico-seconds, two orders of magnitude larger than the ballistic transit time across the devices [7]. Storage times of this magnitude are also suggested by classical simulations of ballistic transport, which properly account for the collimated nature of the incoming particles [12, 23]. In addition, experiment also indicates that electrons trapped in the cavity cool to an effective temperature of at least 50 mK [24]. Combining these considerations to estimate the magnitude of the broadening of the discrete dot levels we obtain a value of 70 mK, which is significantly smaller than the average level spacing of all but the largest cavity studied here (table 1). In other words, by reducing the quantum dot size in experiment, the quantum mechanical nature of transport is expected to become steadily resolved.

Table 1. Transport properties of the devices after illumination at 4.2 K. The carrier density (n_s), mobility (μ), Fermi wavelength (λ_F) and mean free path (l_0) were obtained with the gates grounded. The dot size (L) was inferred from Aharonov–Bohm oscillations at high fields. The cyclotron radius $r_c = \hbar k_F/eB$ and the average level spacing in the dots $\Delta = h^2/2\pi m^* L^2$.

Name	Gate size (μm)	L (μm)	n_s (10^{15} m^{-2})	μ (m^2 V^{-1} s^{-1})	l_0 (μm)	λ_F (nm)	L/λ_F	$2r_c = L$ (T)	Δ/k_B (K)
20A	2.0	1.8	4.9	36	4.2	35	51	0.13	0.03
20B	2.0	1.8	4.8	66	7.6	36	50	0.13	0.03
10A	1.0	0.8	4.9	36	4.2	35	23	0.29	0.13
10B	1.0	0.8	4.8	66	7.6	36	22	0.29	0.13
10C	1.0	0.8	4.5	78	8.7	37	22	0.28	0.13
6A	0.6	0.5	4.8	66	7.6	36	14	0.46	0.33
6B	0.6	0.5	4.5	78	8.7	37	14	0.44	0.33
4A	0.4	0.3	4.5	78	8.7	37	8	0.74	0.92

The samples were mounted in a dilution refrigerator and, unless stated otherwise, low-frequency magneto-transport measurements were made at a refrigerator temperature of 10 mK. A source-drain excitation of less than 3 μV was used for the current-biased measurements, which employ a four-terminal configuration [24]. Over the range of gate voltages of interest here, this resistance is dominated by that of the quantum dot itself.

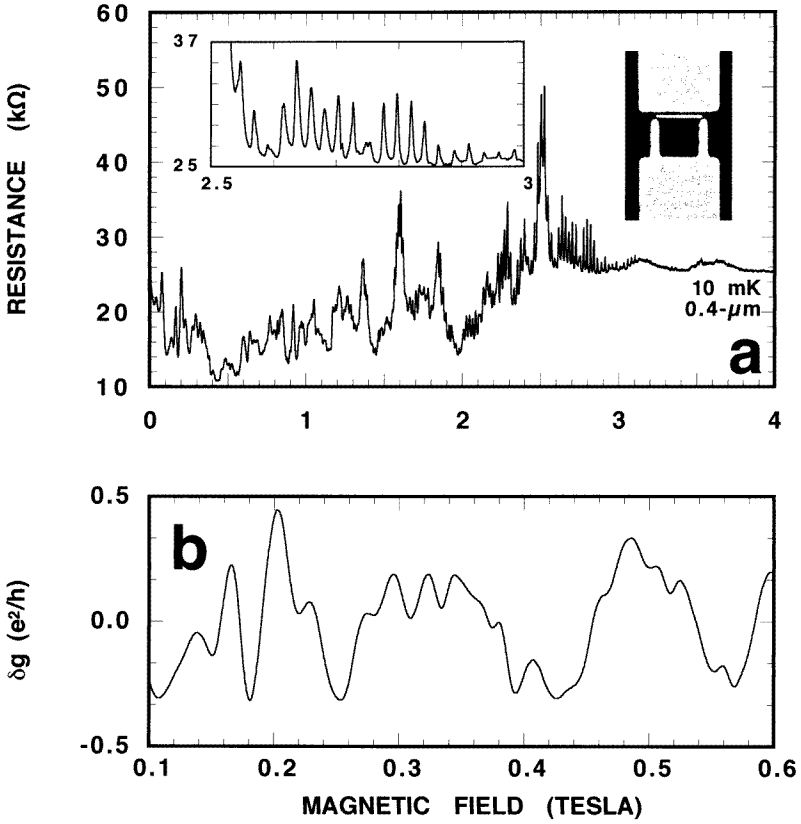

Figure 1. (a) Magneto-resistance of device 4A. Left inset: expanded view of Aharonov–Bohm oscillations in the region from 2.5 to 3 T. Right inset: scanning electron microscope micrograph of a typical device. The spacer bar is 1 μm. (b) Expanded view of the low field fluctuations, obtained on subtracting a polynomial background from the raw data [6].

3. Experimental results

The results of a typical magneto-resistance measurement are illustrated in figure 1. At magnetic fields of order several Tesla, the cyclotron radius of the electrons is significantly smaller than the cavity size and current flows via well defined edge states. In this regime, the periodic Aharonov–Bohm oscillations superimposed on the last quantum Hall plateau result from resonant tunnelling via confined edge states (figure 1(a), left inset) [24–26]. The period of these oscillations can be related to a characteristic area, which in turn provides us with a reliable estimate of the size of the mesoscopic cavity formed in the two-dimensional electron gas (table 1) [24]. Here we are concerned with the behaviour at low magnetic fields, however, where the magneto-resistance is dominated by dense and reproducible fluctuations ($\leqslant$2 T). An expanded view of the fluctuations is shown in figure 1(b), from which it is clear they exhibit a highly periodic nature quite distinct from that of the Aharonov–Bohm oscillations at higher fields. Studying their characteristics as a function of cavity size and gate voltage, the strikingly regular fluctuations are found to be a generic feature of experiment. For example, figure 2(a) shows similar fluctuations for a different gate voltage to that of figure 1, while in figure 2(b) we show the corresponding behaviour in a larger

device. In both of these figures, the periodic nature of the fluctuations is confirmed by the straight line fits obtained on plotting the magnetic field positions of successive fluctuation minima (figures 2(a) and 2(b), upper insets).

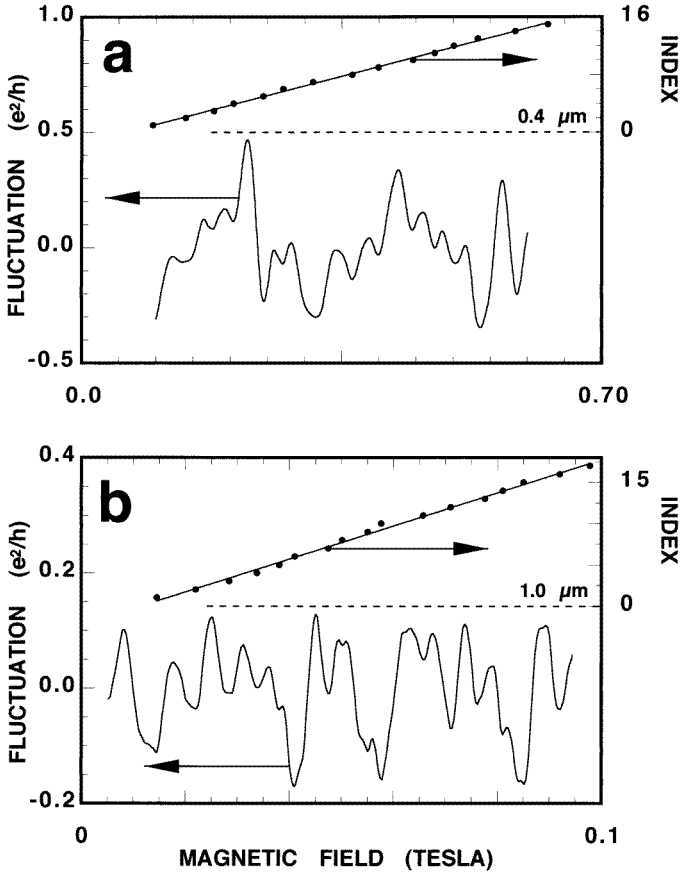

Figure 2. (a) Conductance fluctuations in device 4A for a different gate voltage to that of figure 1. (b) Conductance fluctuations in device 10C. Also shown in the plots are the magnetic field positions of successive fluctuation minima (right-hand axis).

The periodicity of the fluctuations is also confirmed by their Fourier spectra, which typically exhibit well pronounced peaks at a few isolated frequencies (figures 3 and 4). The simple nature of these spectra reflects the underlying periodicity of the raw data and suggests that interference in these devices is dominated by a small number of preferred orbits. An important characteristic of the spectra is the insensitivity of their peak positions to changes in gate voltage, which leads us to suggest that the small group of orbits dominating the interference must be highly stable (figure 3). Closer inspection of the spectra reveals that many of their peaks can be grouped into well defined families of harmonics. According to semi-classical theory, each such family is produced by electrons which undergo multiple traversals of the same closed orbit [2]. These multiple traversals contribute a series of oscillatory terms to the total density of states, which is probed directly in experiment by the application of a magnetic field [16]. Given this interpretation, the spectra shown in figures 3 and 4 are seen to be consistent with just a single orbit dominating transport. The

fundamental frequency of this orbit shows a well defined scaling with dot size, which is best described as a linear dependence on cavity *length* (figure 3, inset), rather than area, an important finding to which we return below.

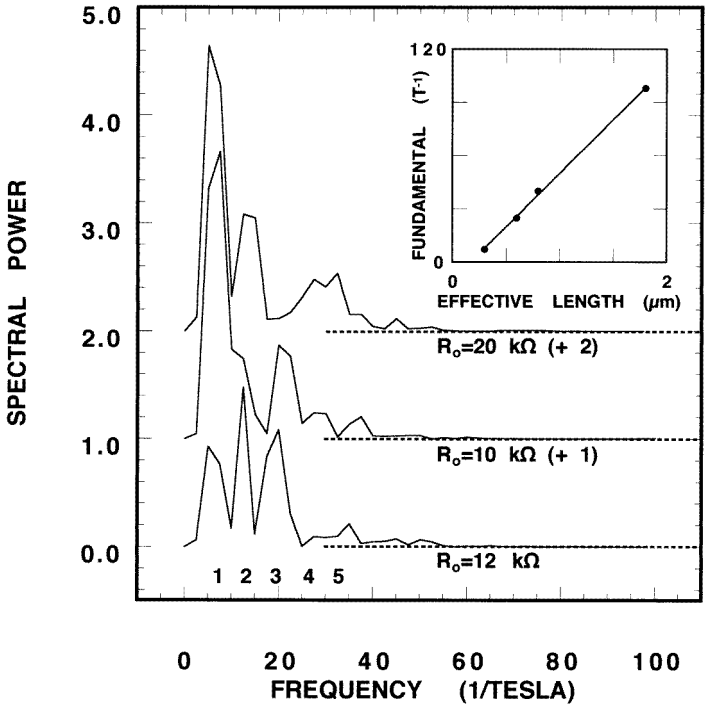

Figure 3. Power spectra of the fluctuations in device 4A. The spectra are labelled by their zero field resistance (R_0), measured after accounting for the effects of weak localization, and exhibit a common fundamental peak. The expected position of successive harmonics is shown at the bottom of the plot. Inset: size-dependent scaling of the fundamental peak in the Fourier spectrum.

A standard approach when discussing the properties of magneto-conductance fluctuations is to define the correlation function [27]:

$$F(\Delta B) = \langle \delta g(B) \cdot \delta g(B + \Delta B) \rangle \tag{1}$$

where $\delta g(B) = g(B) - \langle g(B) \rangle$ and $g(B)$ is the dimensionless conductance at magnetic field B. The angled brackets imply an ensemble average and this is usually assumed to be achieved on averaging over a wide range of magnetic field. A measure of the characteristic field scale of the fluctuations is provided by their correlation field (B_c), in turn defined from the half width of the correlation function:

$$F(B_c) = \frac{F(0)}{2}. \tag{2}$$

A typical correlation function is shown in the inset to figure 4. In this, and all other calculations, each value of the correlation function is obtained by averaging over the same wide range of magnetic field, allowing us to achieve uniform statistics across the entire range of analysis [8]. Features of the correlation function found to be generic to all cases include regions of significant negative excursion and quasi-periodic oscillations in the tail

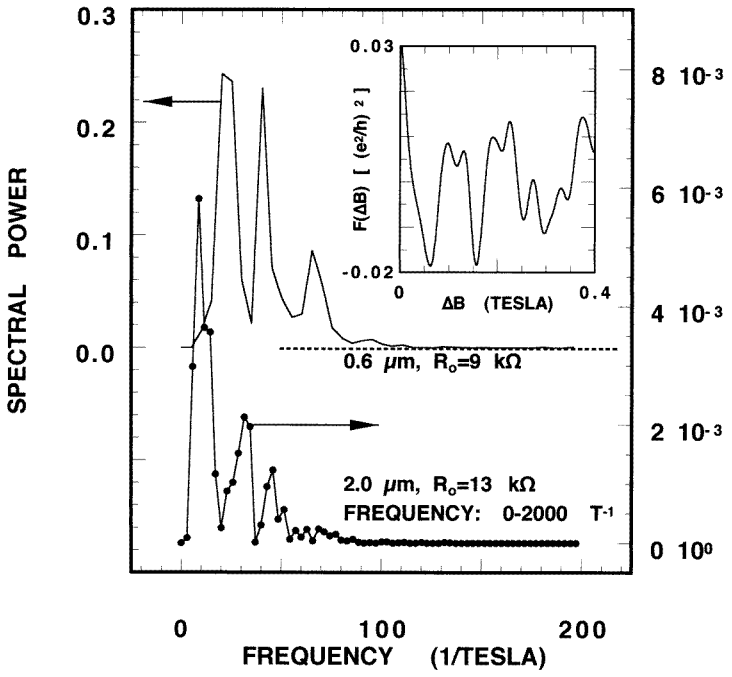

Figure 4. Power spectra of typical fluctuations in devices 6B and 20B. Note that the frequency scale for device 20B runs from 0 to 2000 T^{-1}. Inset: correlation function of the fluctuations for $R_0 = 12$ kΩ.

(figure 4, inset). Recalling that the correlation function of a pure sine wave is simply its corresponding cosine function, the regular oscillations in the tail are again consistent with interference being dominated by a few frequency components. Further evidence for the stability of these components is suggested by studies of the correlation field, which is found to be independent of dot lead opening over the entire range of experiment (figure 5). In disordered systems, the correlation field provides a measure of the characteristic area over which interference occurs [27]. Based on an assumption of chaotic scattering, it has been suggested that this notion can be straightforwardly extended to ballistic quantum dots, in which case the correlation field is expected to show a marked increase as the lead openings are widened [4]. Such behaviour is not apparent here, however, indicating that the quantum dots we study are intrinsically non-ergodic.

Another quantity found to be invariant to changes in lead opening is the fluctuation amplitude (δg_{rms}) (figure 5). Indeed, this quantity is even independent of cavity size, reminiscent of the universal behaviour reported in studies of disordered phase coherent conductors [28]. Motivated by this strong invariance, we construct the ensemble averaged power spectra of the fluctuations by summing over the results of measurements at several gate voltages (figure 6). A clear fundamental peak with weakly resolved harmonics is found to persist on such averaging, consistent with the previously noted insensitivity of the spectral peak positions to changes in gate voltage (figure 3). The amplitude of the fundamental peak increases by more than two orders of magnitude as the dot size is reduced and the discrete energy spectrum of the cavities becomes increasingly resolved (figure 6, right inset), an issue we return to in section 5.

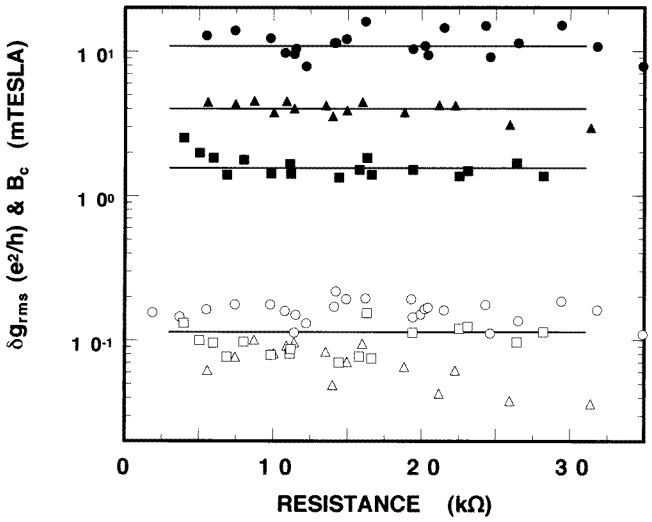

Figure 5. Variation of the correlation field (full symbols) and root-mean-square amplitude (open symbols) of fluctuation with zero field dot resistance. Measurements from three different devices are summarized in this figure: 4A, circles; 6B, triangles; and 10C, squares. The temperature is 10 mK.

On increasing the temperature, the amplitude of the fluctuations is found to be strongly suppressed while the correlation field remains largely unchanged (figures 7 and 8). As was noted in a previous publication [6], this temperature scaling is very different to that of the fluctuations in disordered conductors, in which varying temperature is found to give rise to a well defined change in the fluctuation amplitude and correlation field [27]. In contrast, the independence of the correlation field observed here is yet again suggestive of a fixed set of orbits dominating the interference [4]. As we shall see in the next section, these orbits are manifest through a striking scarring of the electron wavefunction.

4. Comparison to numerical transport simulations

In order to account for our observations, we have performed quantum mechanical simulations of electronic transport in the mesoscopic cavities studied in experiment. These numerical simulations employ a stable iterative matrix technique [29], the details of which have been described elsewhere [12]. The basic idea is that the dot is broken into a series of lattice slices, which are translated across using the transfer matrix, allowing one to evaluate the transmission coefficient of the cavity. The conductance is then obtained from the Landauer–Büttiker formula and we are also able to reconstruct the quantum probability density inside the dot. Connection to experiment is made by choosing the cavity size to account for the known edge-depletion induced around the gates (table 1). Hard-wall conditions are typically assumed, although the effect of realistic potential rounding has also been considered and is found not to significantly affect the conclusions presented here [30]. Finite temperature enters the problem through thermal smearing of the Fermi surface and the phase coherent lifetime of the electrons (τ_ϕ), the latter being accounted for through the use of an imaginary potential [31] ($-\mathrm{i}\hbar/2\tau_\phi$). In this way, we are able to obtain temperature-dependent characteristics consistent with those discussed above [13].

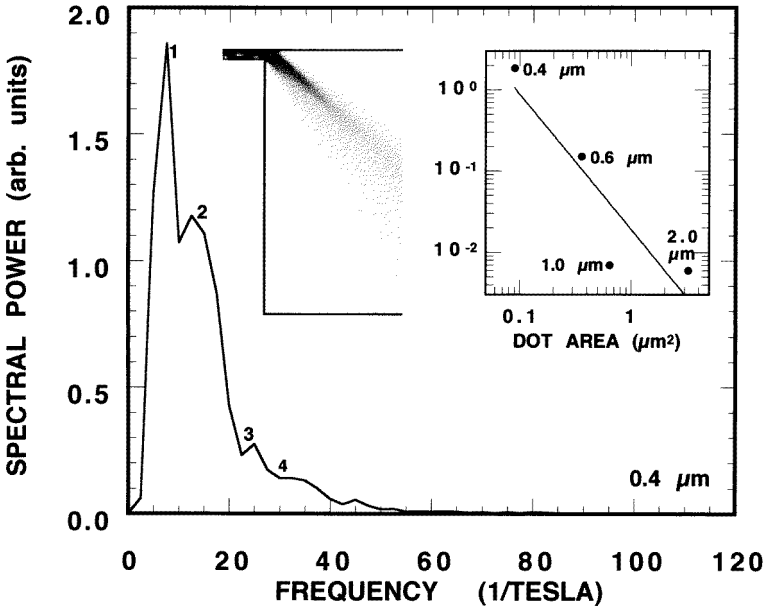

Figure 6. Power spectrum obtained by averaging over 25 different values of R_0 in device 4A. Left inset: wavefunction plot showing collimated beam electrons emerging from the entrance point contact of a 1 μm dot (modelled as 0.8 μm). Three modes are present in the point contact and darker regions correspond to enhanced probability density. Right inset: variation of the fundamental peak's power with dot size. The various data points were obtained by averaging over similarly large numbers of gate voltages to the data shown in the main figure.

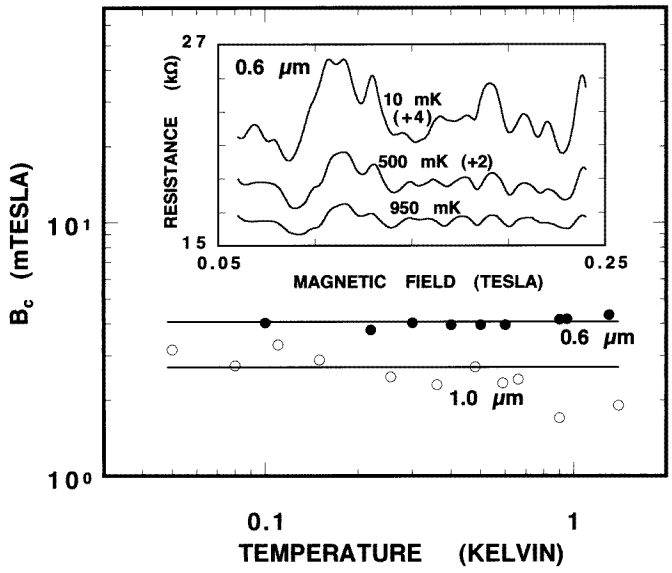

Figure 7. Temperature dependence of the correlation field in devices 10A and 6B. Inset: temperature-dependent decay of the fluctuations in device 6B.

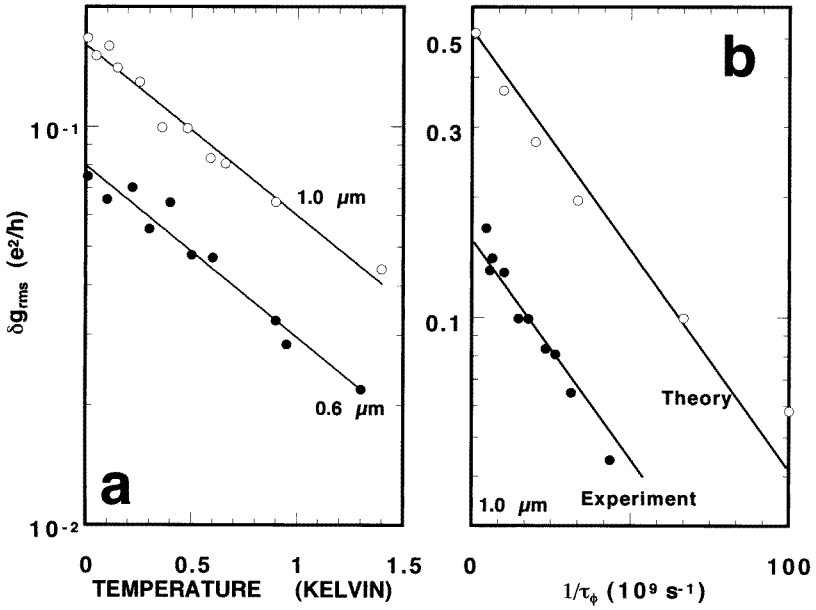

Figure 8. (a) Variation of the root-mean-square amplitude of fluctuation (δg_{rms}) with temperature in devices 10A and 6B. (b) Comparison of the decay of the fluctuation amplitude in a 1 μm dot (modelled as 0.8 μm) as a function of phase breaking rate ($1/\tau_\phi$). In this figure, the experimental values of τ_ϕ were determined by the method of [7].

In figure 9, we show the results of quantum simulations of transport for two different cavity sizes. At absolute zero, and under the assumption of perfect phase coherence, we obtain the magneto-conductance characteristics shown in the insets. As can be seen from figures 9(a) and 9(b), the spectral content of the fluctuations compares very well with that of experiment, particularly at lower frequencies. Differences in high-frequency content between experiment and simulation are thought to reflect the finite temperature at which the former is performed [13]. Nonetheless, it is clear that the simulations account very well for the positions of the major spectral peaks. Turning to the total wavefunction within the cavity, this is found to be strongly scarred by the remnants of a small group of orbits [12, 32–34]. Indeed, for the fluctuations shown in figure 9(b) the scarring is produced by just a single orbit (figure 10(a)), consistent with the results of experiment (figure 3). Further investigations indicate that this scarring recurs periodically in magnetic field, on a field scale which is consistent with the fundamental peak in the Fourier spectrum of the experimental fluctuations [12]. In other words, the periodic fluctuations observed in experiment appear to be associated with wavefunction scarring, produced by the remnants of a small number of orbits. Further calculations reveal a generic feature of this scarring to be its highly stable nature, independent of lead opening or the introduction of realistic rounding to the potential profile [12, 30]. This invariance is consistent with the behaviour in experiment, where the positions of the discrete Fourier peaks and the correlation field of the fluctuations were found to be independent of gate voltage (figures 3 and 5). The scarring also recurs over significant ranges of magnetic field, again consistent with the experimental characteristics of the fluctuations. For example, the diamond feature shown in figure 10(a) can still be seen to recur at fields approaching 0.4 T, where the Lorentz force on the electrons is already significant.

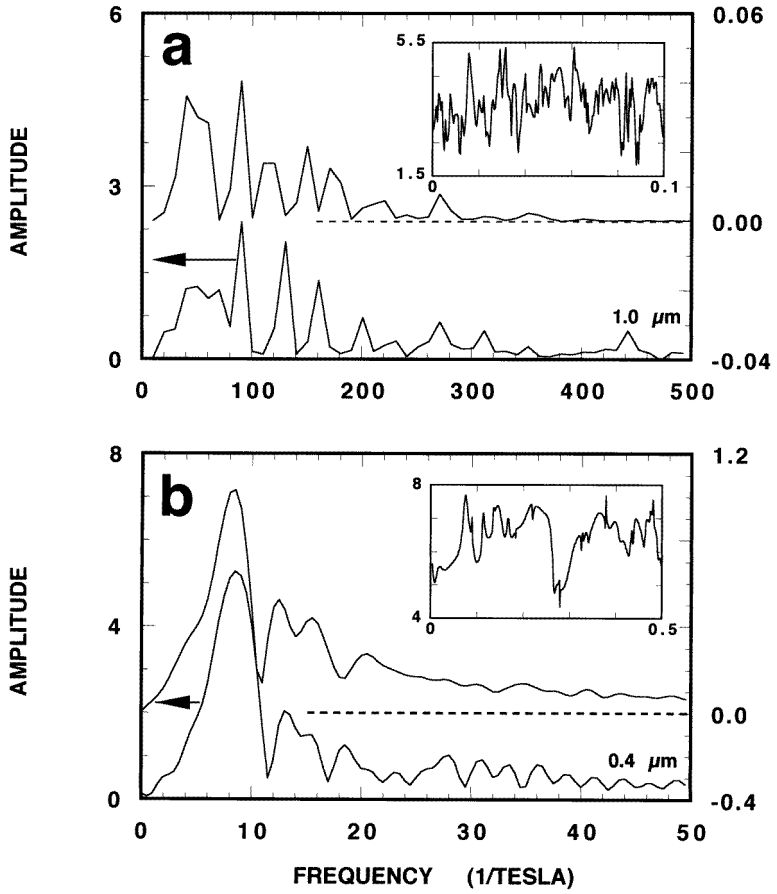

Figure 9. (a) Fourier spectra of the fluctuations in a 1 μm device (modelled as 0.8 μm). The upper curve is obtained from experiment while the lower one is from theory. (b) Fourier spectra of the fluctuations in a 0.4 μm device (modelled as 0.3 μm). The upper curve is obtained from experiment while the lower one is from theory. Insets: typical simulated conductance fluctuations in the devices. Horizontal axis, magnetic field (Tesla); vertical axis, conductance (in units of e^2/h).

Replacing the point contact leads with uniform tunnel barriers, the striking scarring is found to be completely suppressed [12]. In such cases, the wavefunction instead exhibits a uniform sampling of the cavity geometry, indicating that the point contacts play a crucial role in generating the scarring. An important property of the point contacts is known to be their ability to emit electrons in a highly collimated beam [35] (figure 6, left inset). Under conditions of such restricted injection, it is expected that only those cavity eigenstates that efficiently couple to the input beam will participate in transport. This is essentially similar to the situation in resonant tunnelling diodes, in which only those modes which couple effectively to the tunnel barriers are excited to exhibit scars [22] and we have previously argued that the collimation is essential for observation of the scarring [12]. We therefore expect the scarring to be strongly suppressed when the width of the leads is increased such that all cavity modes are uniformly excited by the incoming electrons. This does not seem to occur in experiment, however, where the spectral content of the fluctuations is largely

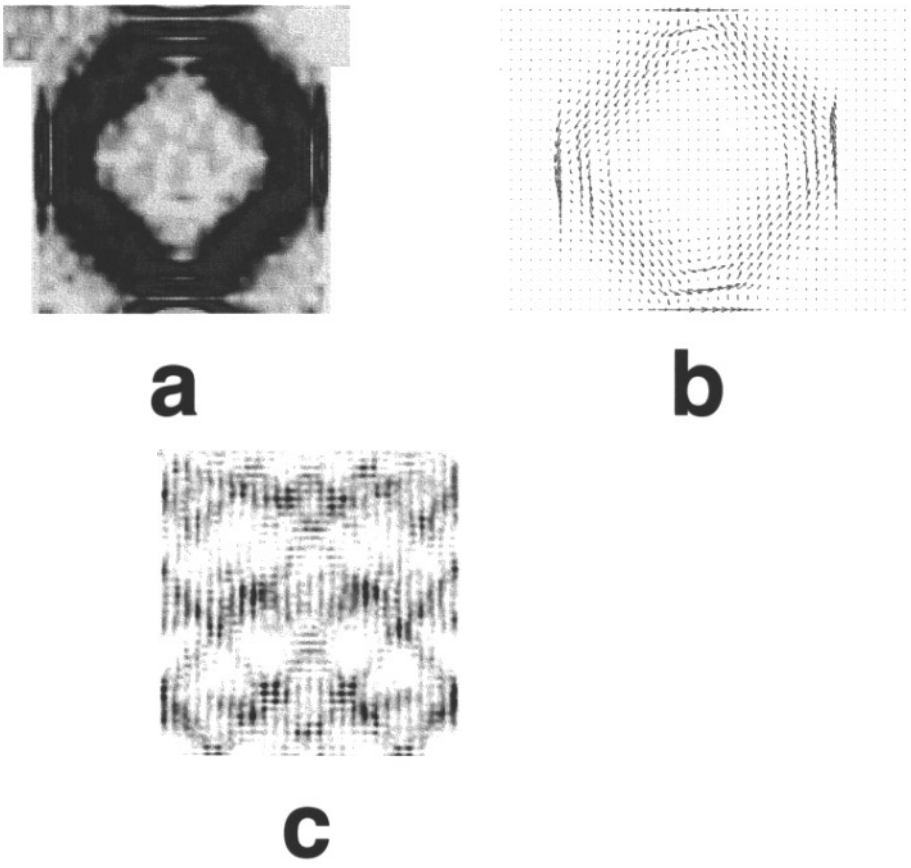

Figure 10. Wavefunction calculations at absolute zero and in the absence of phase breaking (the plots more strictly show the probability density $|\psi(x, y)|^2$. (a) 0.4 μm dot, modelled as a square cavity of side 0.3 μm. Darker regions correspond to enhanced density and the magnetic field is 0.28 T. Three modes are present in the leads. (b) The corresponding probability current distribution for figure 10(a). (c) 1 μm dot, modelled as 0.8 μm. Three modes are present in the leads.

independent of lead opening. Nonetheless, we note from the zero field resistance of the devices that the maximum number of modes in the leads is expected to be of the order of four or five for the range of gate voltages we consider here. Corresponding simulations show that the scarring is still strongly resolved for such mode numbers [12].

Since the calculations presented above are performed at absolute zero, one concern is whether the scarring discussed here can survive under real experimental conditions. On the basis of the good agreement apparent in figure 9, it would seem that the scarring does at least survive to milli-Kelvin temperatures. Its persistence to higher temperatures is a more complex issue, however, the answer to which is provided by the temperature dependence of the phase coherent lifetime. According to a recent numerical study, the scarring is exponentially suppressed in the presence of phase breaking and the amplitude of the fluctuations is similarly reduced [13]. The exponential decay is in very good agreement with that observed in experiment (figure 8(a)), although the absolute values of the computed and experimental fluctuations are found to differ by a temperature independent factor of

roughly four (figure 8(b)). At present, the origin of this discrepancy remains unresolved and an additional, temperature independent, process is required to account for the smaller amplitude found in experiment [13]. One such process might invoke interaction between electrons in the quantum dot and its defining gates [36], while a second-order process involving both the emission and absorption of a plasmon between two dot levels is also possible. At this time, however, we are unable to distinguish between these two distinct processes.

While calculations for larger cavities also reveal the diamond feature apparent in figure 10(a), the scarring in these devices is typically more complex (figure 10(c)). Similarly, the Fourier spectra of their fluctuations are found to exhibit a denser pattern of spectral peaks, associated with the presence of more than one distinct orbit. As we have seen, experiment itself shows a significant suppression in the strength of the periodic fluctuations as the cavity size is increased (figure 6, right inset). These observations are thought to reflect the fact that as the dot size is increased the collimated input beam is able to excite a larger number of cavity eigenstates, which in turn give rise to more complicated scarring characteristics.

5. Discussion and conclusions

In this report, we have considered the nature of ballistic electron transport in open mesoscopic cavities, coupled to external reservoirs by means of few-mode quantum point contacts. The low-temperature magneto-resistance of these devices is found to be characterized by regular fluctuations, associated with the presence of periodically recurring wavefunction scarring. These observations lead us to conclude that the correct semi-classical description of interference in these devices is one in which just a few orbits are excited by the input lead. With a small number of orbits involved in transport, interference occurs whenever the orbits return to their initial point, in this case the injecting point contact [37, 38]. Since experiment is performed in the presence of a weak magnetic field, this causes electrons to precess around the cavity so that many rotations of the quantum dot are required before orbit closure is actually achieved (figure 11, lower inset) [12]. At sufficiently low temperatures, electrons undergo multiple traversals of this basic orbit while maintaining phase coherence and this highly recursive process results in a steady accumulation of probability density. A crucial requirement for the observation of well defined scarring is therefore that electrons remain coherently trapped in the quantum dot over very long time scales [13]. This requirement is reflected in the sensitive temperature dependence of the fluctuations, the amplitude of which is significantly reduced at a few degrees Kelvin, even though the phase coherence length remains an order of magnitude longer than the cavity size (figure 8) [7, 9]. The exponential sensitivity of the fluctuations to temperature is clearly inconsistent with the effects of short orbits [39], but is in very good agreement with the expected behaviour for orbits derived from long classical trajectories [40].

The connection between the semi-classical orbits and the magneto-conductance fluctuations is thought to arise via the density of states. In particular, it has long been recognized that the discrete energy spectrum of a quantum cavity can be decomposed in terms of its associated periodic orbits [41]. Each such orbit contributes an oscillatory term to the total density of states, while multiple traversals of the same orbit yield a series of harmonically related terms [2]. Varying magnetic field sweeps these states through the fixed Fermi level in the external reservoirs, a process which is reflected directly in the magneto-conductance [16]. In the experiment here, the simple periodicity of the fluctuations implies that interference is dominated by a small group of orbits. Since electrons must undergo many rotations of the cavity before orbit closure is achieved, observation of multiple harmonics in

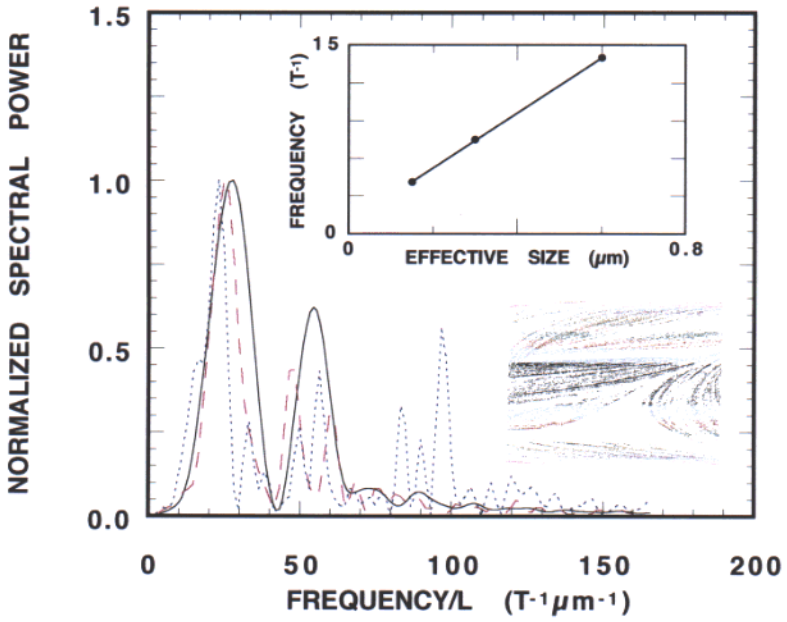

Figure 11. Fourier spectra of the simulated fluctuations for three different cavity sizes: 0.6 μm, dotted curve; 0.3 μm, dashed curve; and 0.15 μm, full curve. In all three cases, the spectra are normalized with regards to their maximum peak height while the frequency is plotted after dividing by the cavity size L. Upper inset: absolute scaling of the fundamental peak frequency with cavity size. Lower inset: the classical Poincaré plot for a magnetic field of 50 mT and an entry angle of 54°, obtained for a limited number of particles injected into a 0.8 μm cavity [12]. Although only a small number of particles has been used so that the discrete trajectory maps are observable, it is clear that the magnetic field induces curvature in the ballistic orbits that causes an apparent phase space filling through precession of the magnetic orbits, even though the motion is fully integrable.

the fluctuation spectra (figures 3 and 4) implies that these orbits must be highly stable. This characteristic is also consistent with the strongly invariant spectral content of the fluctuations, observed in experiment as either temperature (figure 7) or gate voltage (figures 3 and 5) is varied.

The periodic nature of the fluctuations is suppressed in larger cavities, while the scarring is found to weaken and become more complex in nature (figures 6 and 10(c)). These characteristics are thought to reflect the ability of the collimated electrons to excite more eigenstates in larger cavities, in which the average level spacing is correspondingly reduced. A somewhat more surprising observation is that the fundamental frequency of the fluctuations scales as a linear function of cavity size (figure 3, inset). This dependence is confirmed by the results of simulations (figure 11), indicating that the field scale for recurrence of a particular scar is *not* determined by the area which the scar itself encloses. Rather, it is the symplectic area which the underlying classical orbit sweeps out which is important. In order to appreciate how the length-dependent scaling might arise, recall the precessing motion of semi-classical electrons which gives rise to the observed scarring. The magnetic flux enclosed by each such orbit is directly proportional to its symplectic area, which in turn is quite distinct from the scalar area enclosed by its boundary [42]. In

particular, since the electrons typically undergo many traversals of the dot before closing their orbit, it is the net area enclosed between these traversals which is important. From studies of universal conductance fluctuations in disordered systems, it is known that the symplectic area enclosed between two different trajectories scales in proportion to their length [27]. The length-dependent scaling we observe here appears consistent with these arguments, suggesting that a particular scar recurs whenever the flux threading the symplectic area of its underlying orbit increases by one quantum.

While the quantum dots we study here are fabricated with a regular lithographic geometry, the negative bias applied to the surface gates may ultimately render the shape of the electrostatically defined cavity chaotic (this is particularly true of the smallest dots we study). Numerical studies indicate that the scarring we consider here persists in such cases [30], however, in accordance with which we note that periodic fluctuations have also been observed in mesoscopic stadia, the classical dynamics of which is known to be chaotic [3, 43]. The scarring implies a non-uniform sampling of phase space within the cavity, behaviour which is quite at odds with the uniform phase space filling expected for chaotic dynamics. We therefore conclude that chaotic scattering is suppressed in mesoscopic cavities, regardless of the underlying classical dynamics, once their discrete quantum mechanical nature becomes sufficiently resolved. In these devices, transport instead occurs via a small number of regular orbits, which are stabilized by the role of the quantum point contact leads and the discrete quantization within the cavity itself. These long orbits give rise to well defined wavefunction scarring with measurable magneto-transport results.

Acknowledgments

JPB would like to sincerely thank H Hanami for invaluable experimental assistance. Work at ASU was supported in part by ONR.

References

[1] Casati G and Chirikov B (eds) 1995 *Quantum Chaos* (Cambridge: Cambridge University Press)
[2] Ozorio de Almeida A M 1988 *Hamiltonian Systems: Chaos and Quantization* (Cambridge: Cambridge University Press)
[3] Marcus C M, Rimberg A J, Westervelt R M, Hopkins P F and Gossard A C 1992 *Phys. Rev. Lett.* **69** 506
[4] Marcus C M, Westervelt R M, Hopkins P F and Gossard A C 1993 *Phys. Rev.* B **48** 2460
Clarke R M, Chan I H, Marcus C M, Duruöz C I, Harris J S Jr, Campman K and Gossard A C 1995 *Phys. Rev.* B **52** 2656
[5] Chang A M, Baranger H U, Pfeiffer L N and West K W 1994 *Phys. Rev. Lett.* **73** 2111
[6] Bird J P, Ishibashi K, Aoyagi Y, Sugano T and Ochiai Y 1994 *Phys. Rev.* B **50** R18 678
[7] Bird J P, Ishibashi K, Ferry D K, Ochiai Y, Aoyagi Y and Sugano T 1995 *Phys. Rev.* B **51** R18 037
[8] Bird J P, Ferry D K, Akis R, Ochiai Y, Ishibashi K, Aoyagi Y and Sugano T 1996 *Europhys. Lett.* **35** 529
[9] Connolly K M, Pivin D P, Ferry D K and Wieder H H 1996 *Superlatt. Microstruct.* **20** 307
[10] Stopa M 1996 *Phys. Rev.* B **53** 9595
Stopa M 1996 *Phys. Rev.* B **54** 13 767
[11] Richter K, Ullmo D and Jalabert R A 1996 *Phys. Rev.* B **54** R5219
[12] Akis R A, Ferry D K and Bird J P 1996 *Phys. Rev.* B **54** 17 705
[13] Akis R A, Bird J P and Ferry D K 1996 *J. Phys.: Condens. Matter* **8** L667
[14] Akis R A, Ferry D K and Bird J P 1997 *Phys. Rev. Lett.* accepted for publication
[15] Wang Y, Zhu N, Wang J and Guo H 1996 *Phys. Rev.* B **53** 16 408
Wang J, Wang Y and Guo H 1994 *Appl. Phys. Lett.* **65** 1793
[16] Berggren K F, Ji Z L and Lundberg T 1996 *Phys. Rev.* B **54** 11 612
[17] Jalabert R A, Baranger H U and Stone A D 1990 *Phys. Rev. Lett.* **65** 2442
[18] Baranger H U, Jalabert R A and Stone A D 1993 *Phys. Rev. Lett.* **70** 3876

[19] Baranger H U and Mello P A 1995 *Phys. Rev. Lett.* **73** 142
[20] Baranger H U and Mello P A 1995 *Phys. Rev.* B **51** R4703
[21] Fromhold T M, Eaves L, Sheard F W, Leadbetter M L, Foster T J and Main P C 1994 *Phys. Rev. Lett.* **72** 2608
[22] Fromhold T M, Wilkinson P B, Sheard F W, Eaves L, Miao J and Edwards G 1995 *Phys. Rev. Lett.* **75** 1142
[23] Ferry D K and Edwards G 1997 *VLSI Design* at press
[24] Bird J P, Stopa M, Ishibashi K, Aoyagi Y and Sugano T 1994 *Phys. Rev.* B **50** 14 983
[25] van Wees B J, Kouwenhoven L P, Harmans C J P M, Williamson J G, Timmering C E, Broekaart M E I, Foxon C T and Harris J J 1989 *Phys. Rev. Lett.* **62** 2523
[26] Stopa M, Bird J P, Ishibashi K, Aoyagi Y and Sugano T 1996 *Phys. Rev. Lett.* **76** 2145
[27] Ferry D K and Goodnick S M 1997 *Transport in Nanostructures* (Cambridge: Cambridge University Press) at press
[28] Washburn S and Webb R A 1986 *Adv. Phys.* **35** 375
[29] Usuki T, Saito M, Takatsu M, Keihl R A and Yokoyama N 1995 *Phys. Rev.* B **52** 8244
[30] Akis R, Ferry D K and Bird J P 1997 *Japan. J. Appl. Phys.* at press
[31] Wang Y, Wang J and Guo H 1993 *Phys. Rev.* B **47** 4348
[32] Heller E J 1984 *Phys. Rev. Lett.* **53** 1515
[33] Berry M V 1989 *Proc. R. Soc., London* A **423** 219
[34] Bogolmolny E B 1988 *Physica* D **31** 169
[35] Beenakker C W J and van Houten H 1991 *Solid State Physics* **44** 1
[36] Marcus C Private communication
[37] Berry M V 1984 *The Wave–Particle Dualism* ed S Diner *et al* (Dordrecht: Riedel)
[38] Grincwajg A, Ferry D K and Edwards G 1996 *Physica* B **218** 92
[39] Baranger H U and Mello P A 1996 *Europhys. Lett.* **33** 465
[40] Berry M V and Mount K E 1972 *Rept. Prog. Phys.* **35** 315
[41] Gutzwiller M C 1971 *J. Math. Phys.* **12** 343
Balian R and Bloch C 1974 *Ann. Phys.* **85** 514
Berry M V and Tabor M 1976 *Proc. R. Soc., London* A **349** 101
Berry M V and Tabor M 1977 *J. Phys. A: Math. Gen.* **10** 371
[42] Beenakker C W J and van Houten H 1988 *Phys. Rev.* B **37** 6544
de Gennes P G and Tinkham M 1964 *Physics* **1** 107
[43] Okubo Y, Bird J P, Ochiai Y, Ferry D K, Ishibashi K, Aoyagi Y and Sugano T 1997 *Phys. Rev.* B **54** 1368